

# Modelling flows within forested areas using the $k-\varepsilon$ RaNS model

A Silva Lopes<sup>1</sup>, J M L M Palma<sup>1</sup> and J Viana Lopes<sup>2</sup>

<sup>1</sup> Faculdade de Engenharia da Universidade do Porto  
Rua Dr. Roberto Frias s/n, 4200-465 Porto, Portugal

<sup>2</sup> Faculdade de Ciências da Universidade do Porto  
Rua do Campo Alegre 687, 4169-007 Porto, Portugal

E-mail: asl@fe.up.pt

**Abstract.** A new canopy model for the Reynolds-averaged Navier-Stokes (RaNS) method with the  $k-\varepsilon$  turbulence model was developed. To derive the effect of vegetation on the transport of turbulent quantities, it uses a Taylor series expansion of the velocity magnitude, which is part of the definition of the canopy drag force, and assumes that the turbulent kinetic energy is much smaller than the kinetic energy of the mean flow. The resultant model is composed by a sum of velocity moments of increasing order. Initially, it was expected that truncating the sum at low-order, including only terms that can be expressed using quantities available within the  $k-\varepsilon$  RaNS model, would provide better accuracy than traditional models, based mainly on dimensional arguments. However, the results obtained with this approach mimic those obtained with a model based on dimensional arguments and calibrated using results of large-eddy simulations, proving the validity of both approaches and showing that the accuracy in the modelling of the flows over vegetation is limited by the  $k-\varepsilon$  model itself and not by the modelling of vegetation effects on turbulence.

## 1. Introduction

Vegetation covers a substantial part of the Earth's surface and affects considerably the turbulence on the flows over it: usually, a high shear is found near the top of the vegetation, which results in high turbulence production, while the large-scales are broken in the flow inside, increasing the turbulence dissipation. Appropriate modelling of these features is obviously important in the study of many atmospheric flows and, particularly, in numerical models used in wind-energy engineering: higher shear means that a wind turbine will withstand increased fatigue, will also increase turbulence production and, consequently, fluctuations in power output. However, higher turbulence means also increased mixing, faster recovery in the wake and changes in the optimal wind-farm layout. Although, despite being the subject of many studies [1–4], a consensus about the appropriate model for vegetation effects on turbulence has not yet been reached.

Most models look at the vegetation as a porous media and add a drag force to the momentum transport equation. Within the  $k-\varepsilon$  model, the effect on turbulent quantities is accounted with additional terms on the transport equations,

$$F_k^{k-\varepsilon} = C_z (\beta_p |\mathbf{U}|^3 - \beta_d |\mathbf{U}|k) , \quad (1a)$$



$$\mathcal{F}_\varepsilon^{k-\varepsilon} = C_z \left( C_{\varepsilon 4} \beta_p |\mathbf{U}|^3 \frac{\varepsilon}{k} - C_{\varepsilon 5} \beta_d |\mathbf{U}| \varepsilon \right), \quad (1b)$$

where  $F_k$  and  $\mathcal{F}_\varepsilon$  are the contributions to the  $k$  and  $\varepsilon$  transport equations,  $C_z = C_d a(z)$  is the product of the drag coefficient by the leaf area density,  $|\mathbf{U}|$  is the magnitude of the mean velocity and  $\beta_p$ ,  $\beta_d$ ,  $C_{\varepsilon 4}$  and  $C_{\varepsilon 5}$  are the model coefficients, specific to each model. In  $F_k$ , the former term, proportional to  $U^3$ , represents additional production due to shear; the latter, proportional to  $U \cdot k$ , accounts for enhanced dissipation due to the breaking of the large-scales into smaller ones.  $\mathcal{F}_\varepsilon$  is similar to  $F_k$ , with each term divided by the time-scale  $\tau = k/\varepsilon$ . The coefficients are usually obtained by optimization of mean velocity, turbulent kinetic energy (TKE) or Reynolds shear stress profiles [1, 3], but they were also determined using analytical [4] and large-eddy simulation results [5].

Here, a different approach was used. Starting with the same treatment of the vegetation as a porous media and assuming that the TKE is smaller than the kinetic energy of the mean flow, the perturbation theory was used to expand the velocity magnitude around a velocity scale based on the total kinetic energy of the flow (mean flow + turbulence). This allowed to express the terms that represent the canopy effect on turbulent quantities as a sum of velocity moments, where the low-order terms use quantities available within the  $k-\varepsilon$  model. Large-eddy simulations of three flows with increasing complexity—a horizontally homogeneous canopy, a forest edge and a forested hill—were used in an *a priori* assessment of the model and *a posteriori* results were compared to the same large-eddy simulations and to a reference model, based on eqs. (1).

## 2. Mathematical Model

A neutrally stratified atmospheric flow is governed by the equations expressing the conservation of mass and momentum, either filtered (LES) or time-averaged (RaNS),

$$\frac{\partial \bar{u}_i}{\partial x_i} = 0, \quad (2a)$$

$$\frac{\partial \bar{u}_i}{\partial t} + \frac{\partial (\bar{u}_j \bar{u}_i)}{\partial x_j} = -\frac{1}{\rho} \frac{\partial \bar{p}}{\partial x_i} + \nu \frac{\partial^2 \bar{u}_i}{\partial x_j \partial x_j} - \frac{\partial \tau_{ij}}{\partial x_j} + f_i^{\text{can}}, \quad (2b)$$

where  $u_i$  is the component of the velocity in the Cartesian direction  $x_i$  ( $i = 1, 2, 3$  or  $x_i = x, y, z$ ),  $p$  is the pressure,  $\rho$  and  $\nu$  are the standard air density and kinematic viscosity. The overline denotes a filtered (LES) or a time-averaged quantity (RaNS). In LES,  $\tau_{ij} = \bar{u}_i u_j - \bar{u}_i \bar{u}_j$  are the subgrid stresses, while in RaNS,  $\tau_{ij} = \overline{u'_i u'_j}$  are the Reynolds stresses. Both were modelled using an eddy-viscosity assumption.  $f_i^{\text{can}}$  represents the drag force due to the canopy and will be detailed in section 3.

### 2.1. LES Subgrid Model

In the large-eddy simulations, the anisotropic part of the subgrid stress was determined using an eddy-viscosity assumption,

$$\tau_{ij} - \frac{1}{3} \delta_{ij} \tau_{kk} = -2\nu_t \bar{S}_{ij} = -2(C\bar{\Delta})^2 |\bar{S}| \bar{S}_{ij}, \quad (3)$$

where  $\bar{\Delta} = (\Delta x \Delta y \Delta z)^{1/3}$  is the filter size,  $\bar{S}_{ij} = (\partial \bar{u}_i / \partial x_j + \partial \bar{u}_j / \partial x_i) / 2$  is the resolved strain-rate tensor and  $|\bar{S}| = (2\bar{S}_{ij} \bar{S}_{ij})^{1/2}$  is its magnitude. The coefficient  $C$  was determined using a combination of a wall-damped Smagorinsky model near the surface [6] and, far away, the Lagrangian dynamic model [7]. The models merged below  $0.75h$  and  $C_S = 0.16$  was used in the Smagorinsky model. This combination avoids the underdissipative character of the dynamic model near the surface, which can cause unrealistic oscillations and decoupling of the velocity and pressure fields. Further details about the model can be found in Silva Lopes *et al* [5].

## 2.2. RaNS $k-\varepsilon$ Model

The  $k-\varepsilon$  turbulence model has two additional transport equations, for the turbulent kinetic energy,  $k = \overline{u'_i u'_i} / 2$ , and its dissipation rate,  $\varepsilon$ ,

$$\frac{Dk}{Dt} = \frac{\partial}{\partial x_j} \left[ \left( \nu + \frac{\nu_T}{\sigma_k} \right) \frac{\partial k}{\partial x_j} \right] + \mathcal{P}_k - \varepsilon + F_k^{k-\varepsilon}, \quad (4a)$$

$$\frac{D\varepsilon}{Dt} = \frac{\partial}{\partial x_j} \left[ \left( \nu + \frac{\nu_T}{\sigma_\varepsilon} \right) \frac{\partial \varepsilon}{\partial x_j} \right] + C_{\varepsilon 1} \frac{\varepsilon}{k} \mathcal{P}_k - C_{\varepsilon 2} \frac{\varepsilon^2}{k} + \mathcal{F}_\varepsilon^{k-\varepsilon}, \quad (4b)$$

where  $\mathcal{P}_k = -\overline{u'_i u'_j} \partial \bar{u}_i / \partial x_j$  is the TKE production. Eddy viscosity is calculated from  $\nu_T = C_\mu k^2 / \varepsilon$  and Reynolds stresses are given by

$$\tau_{ij} - \frac{2}{3} \delta_{ij} k = -2\nu_T \bar{S}_{ij}. \quad (5)$$

The standard coefficients of the model [8] were used here:

$$C_\mu = 0.09, \quad C_{\varepsilon 1} = 1.44, \quad C_{\varepsilon 2} = 1.92, \quad \sigma_k = 1.0, \quad \sigma_\varepsilon = 1.3.$$

This set of coefficients provided a better agreement between LES and RaNS in the base configuration (the horizontally homogeneous canopy) than the set suggested by Beljaars *et al* [9] for the simulation of atmospheric flows.

$F_k^{k-\varepsilon}$  and  $\mathcal{F}_\varepsilon^{k-\varepsilon}$  are the counterpart of the canopy drag  $f_i^{\text{can}}$  in the  $k$  and  $\varepsilon$  transport equations and their modelling is the subject of section 3. Their exact definitions are obtained similarly to the other terms in these transport equations,

$$\begin{aligned} \overline{u'_i \frac{Du'_i}{Dt}} &= \frac{1}{2} \overline{\frac{Du'_i u'_i}{Dt}} = \frac{Dk}{Dt} = \dots + F_k, \\ 2\nu \overline{\frac{\partial u'_i}{\partial x_k} \frac{D}{Dt} \left[ \frac{\partial u'_i}{\partial x_k} \right]} &= \frac{D}{Dt} \nu \overline{\frac{\partial u'_i}{\partial x_k} \frac{\partial u'_i}{\partial x_k}} = \frac{D\varepsilon}{Dt} = \dots + \mathcal{F}_\varepsilon, \end{aligned}$$

where

$$F_k = \overline{u'_i f_i^{\text{can}}}, \quad \mathcal{F}_\varepsilon = 2\nu \overline{\frac{\partial u'_i}{\partial x_k} \frac{\partial f_i^{\text{can}}}{\partial x_k}}.$$

## 2.3. Physical Domain and Boundary Conditions

To test the canopy model, three flow configurations were considered, all with detailed results previously published: the flow over a horizontally homogeneous canopy [10], a forest edge [11] and a forested hill [12]. All used periodic conditions in the streamwise and spanwise directions, the wall-model of Marusic *et al* [13] at the bottom rough surface and a free-slip condition at the top. The streamwise pressure gradient was calculated at each timestep to maintain a constant average wind speed  $U_b$  and table 2.3 lists the specific details of each case. The grids used a hyperbolic tangent stretching near the canopy top, with maximum expansion factor lower than 1.1 and maximum vertical space not much larger than the horizontal ( $\Delta z_{\text{max}} < 1.1\Delta x$ ). The large-eddy simulations were previously validated [5] and RaNS simulations used the same grid, while in wind-engineering applications they will, most likely, use a coarser resolution.

**Table 1.** Specific details of each test case.

	Homogeneous	Forest edge	Forested hill
Domain size	$9.6h \times 4.8h \times 3.0h$	$38.4h \times 19.2h \times 6.2h$	$300h \times 60h \times 20h$
Grid nodes	$192 \times 96 \times 98$	$480 \times 240 \times 101$	$849 \times 170 \times 125$
$\Delta x/h = \Delta y/h$	$5.00 \times 10^{-2}$	$8.00 \times 10^{-2}$	$3.5 \times 10^{-1}$
$\Delta z_{\min}/h$	$1.25 \times 10^{-2}$	$1.07 \times 10^{-2}$	$3.5 \times 10^{-2}$
$h$ (m)	20	7.5	3.0
$U_b$ (m/s)	2	3	2
$z_0/h$	$1.00 \times 10^{-3}$	$3.73 \times 10^{-3}$	$3.0 \times 10^{-3}$
$C_d$	0.15	0.2	0.2
$LAI$	2.0	2.0	1.6

### 3. Canopy Model

Numerical modelling of the vegetation as a porous media considers a drag force,

$$f_i^{\text{can}} = -C_d a(z) |\mathbf{u}| u_i, \quad (6)$$

where  $C_d$  is a mean drag coefficient and  $a(z)$  is the leaf area density ( $LAD$ ). The drag coefficient  $C_d$  can be considered constant if the pressure (form) drag is much larger than the viscous drag, which is the case for flows considered here. A  $LAD$  profile representative of a deciduous forest with a relatively open trunk space [10] was assumed.

All the canopy-related terms in the transport equations depend on the velocity magnitude. Using a velocity scale  $Q = (U^2 + 2k)^{1/2}$ , based on the sum of the kinetic energies of the mean flow and turbulence, and assuming that the turbulent fluctuations  $u'_i$  are much smaller than the mean-flow velocity, i.e.  $u'_i u'_i \ll U^2$ , an approximation for  $|\mathbf{U}|$  based on the perturbation theory was obtained,

$$|\mathbf{U}| = Q \sqrt{1 + 2 \frac{U u'_s}{Q^2} + \frac{u'_i u'_i - 2k}{Q^2}}, \quad (7)$$

where  $u'_s$  is the velocity fluctuation along the streamline direction. Performing a Taylor series expansion of the square root, using  $\xi = U u'_s / Q^2$  and  $\eta = (u'_i u'_i - 2k) / Q^2$ ,

$$\sqrt{1 + 2\xi + \eta} \approx 1 + \xi + \frac{\eta - \xi^2}{2} + \frac{\xi^3 - \xi\eta}{2} + \frac{6\xi^2\eta - \eta^2 - 5\xi^4}{2} + \dots, \quad (8)$$

which expresses the velocity magnitude as a sum of velocity moments with increasing order (see Viana Lopes *et al* [14] for further details). An important part of this deduction was assuming that the turbulent fluctuations were much smaller than the mean flow velocity, which we will call here the weak turbulence regime (WTR). While in our large-eddy simulation of the flow inside the horizontally homogeneous canopy the turbulence intensity was always lower than 45%, the approximation can be questionable near the ground or when the flow separates. However, as will be shown, the resultant model proved to be robust.

A similar approach is used by Lien *et al* [15], but with the magnitude of the mean flow velocity as velocity scale. However, that approximation should be less robust when the mean velocity is small as, for instance, inside the separated region in the lee side of the flow over the forested hill.

Although the canopy drag can be directly modelled in RaNS with (6), it does not yield the same time-averaged force than when applied within LES methods, since  $|\overline{\mathbf{u}}| \overline{u_i} \leq \overline{|\mathbf{u}| u_i}$ . To

increase the agreement with LES, we used the WTR expansion (8) to obtain the canopy drag, expressed as a sum of terms with decreasing order of magnitude,

$$\overline{f_i^{\text{can}}} = -C_d a(z) \overline{|\mathbf{u}| u_i} \approx S_{U_i}(n) = -C_d a(z) \sum_{j=0}^n s_{U_i}(j), \quad (9)$$

where the first four terms of the expansion are

$$s_{U_i}(0) = Q U_i, \quad (10a)$$

$$s_{U_i}(1) = 0, \quad (10b)$$

$$s_{U_i}(2) = \frac{U}{Q} \left( \overline{u'_i u'_s} - \frac{U U_i}{2Q^2} \overline{u'_s u'_s} \right), \quad (10c)$$

$$s_{U_i}(3) = \frac{1}{2Q} \left( \overline{u'_i u'_j u'_j} - \frac{U^2}{Q^2} \overline{u'_i u'_s u'_s} \right). \quad (10d)$$

With this approach, starting with the second-order  $s_{U_i}(2)$ , there is an average finite drag when the mean velocity becomes small ( $U \rightarrow 0$ ), due to the turbulent fluctuations, and a small drag normal to the flow direction if the two velocity components are correlated, i.e. the Reynolds shear stress  $\overline{u'_s u'_n}$  is not null ( $u'_n$  is the velocity fluctuation in the direction normal to the streamline). Although the normal component is much smaller than the streamwise component, this is a relevant formal difference between the two approaches.

The WTR Taylor series expansion of the velocity magnitude was also used to obtain the canopy effect on the TKE transport as a sum of terms with decreasing order of magnitude,

$$F_k = \overline{u'_i f_i^{\text{can}}} = -C_d a(z) \overline{|\mathbf{u}| u_i u'_i} \approx -C_d a(z) \sum_{l=0}^n s_k(l), \quad (11)$$

where the first terms of the expansion are

$$s_k(0) = 2 Q k, \quad (12a)$$

$$s_k(1) = 0, \quad (12b)$$

$$s_k(2) = \frac{U^2(Q^2 - k)}{Q^3} \overline{u'^2_s}, \quad (12c)$$

$$s_k(3) = \frac{U(3Q^2 - 2k)}{2Q^3} \overline{u'_s u'_i u'_i} - \frac{U^5}{2Q^5} \overline{u'^3_s}, \quad (12d)$$

$$s_k(4) = \frac{U^4(2Q^2 - 5k)}{4Q^7} \overline{u'^4_s} - \frac{U^2(2Q^2 - 3k)}{2Q^5} \overline{u'^2_s (u'^2_i - 2k)} + \frac{2Q^2 - k}{4Q^3} \left[ \overline{u'^4_i} - 4k^2 \right]. \quad (12e)$$

In both cases ( $\overline{f_i^{\text{can}}}$  and  $F_k$ ), the series are sums of time-averaged velocity moments. Truncating them to second-order provides approximations for  $\overline{f_i^{\text{can}}}$  and  $F_k$  requiring only quantities that can be obtained within standard RaNS models. Using an approximation for the third-order correlations, third-order terms can also be used with the  $k-\varepsilon$  model. One of such approximations was proposed by Daly and Harlow [16]:

$$\overline{u'_i u'_j u'_k} \approx -C_S \frac{k}{\varepsilon} \overline{u'_k u'_\ell} \frac{\partial \overline{u'_i u'_j}}{\partial x_\ell}, \quad (13)$$

where we used  $C_S = 0.22$ . This approximation for the turbulent effect on the TKE transport should provide better accuracy than the models based on eqs. (1) when the flow is not in equilibrium, such as when it is accelerating or decelerating.

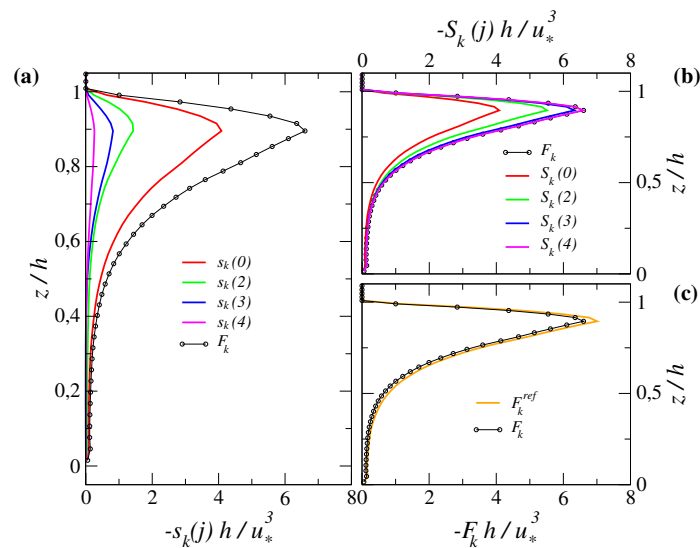


**Figure 1.** Canopy drag effect on the TKE transport in the flow over a horizontally homogeneous forest: (a)  $n$ th-order terms of the series approximation ( $s_k(n)$ ), (b) approximation using terms up to the  $n$ th-order ( $S_k(n)$ ) and (c) reference RaNS model ( $F_k^{ref}$ ). Canopy drag effect determined with large-eddy simulation ( $F_k$ ) is shown also for comparison.

The same approach could also be used for the effect of the vegetation drag on the TKE dissipation rate transport,  $\mathcal{F}_\varepsilon$ . However, here we simply related it with  $F_k$ , using the time-scale  $\tau = k/\varepsilon$ , as it is done with many other models [1–5] and other terms of the transport equation for  $\varepsilon$ :  $\mathcal{F}_\varepsilon^{k-\varepsilon} \approx C_{\varepsilon 5} F_k^{k-\varepsilon} / \tau$ , where the coefficient  $C_{\varepsilon 5} = 0.9$  was previously found from large-eddy simulation results [5].

#### 4. Results and Discussion

To test the accuracy of the new model, an *a priori* assessment was performed, using results of the flow over a horizontally homogeneous canopy. With this comparison, the merit of the model can be judged by itself, without the influence of any  $k-\varepsilon$  model limitation.

A second test involved an *a posteriori* comparison of the model with large-eddy simulation results that were previously validated and with a reference RaNS canopy model, based on the dimensional arguments of eqs. (1) and with  $\beta_d = 4.0$ ,  $C_{\varepsilon 5} = 0.9$  and  $\beta_p = C_{\varepsilon 4} = 0$  [5]. These coefficients were calibrated using large-eddy simulation results and were found to depend weakly on the flow configuration. Three different flow configurations, with increasing complexity, were used: the flow over a horizontally homogeneous canopy, a forest edge and a forested hill.

##### 4.1. A Priori Assessment

*A priori* tests intended to verify that the WTR canopy model was able to predict the contribution to the TKE transport when provided with the correct flow statistics, obtained from large-eddy simulations. Although the model was tested in different flow configurations [14], here we show only the results for the flow over a horizontally homogeneous canopy. The analysis of the first four orders of the WTR expansion shows the convergence of the series, since the magnitude decreases with the increasing order of the term (figure 1a). The second-order approximation had a similar accuracy than the reference model, accounting for at least 80% of the vegetation effect, while the inclusion of the third-order term was sufficient to capture 97% of the large-eddy simulation results (figure 1b).

#### 4.2. A Posteriori Comparison

The *a posteriori* tests compare results of numerical simulations using the WTR and reference canopy models with large-eddy simulations. Comparing with the *a priori* assessment, here what is evaluated is the accuracy of the WTR canopy model when part of a RaNS  $k-\varepsilon$  model simulation, and not only the canopy model.

In the flow over a horizontally homogeneous canopy, the WTR models predicted accurately the velocity profile (figure 2a) and improved the TKE profile, attenuating the underprediction of TKE near the ground that is one of the deficiencies of the reference model (figure 2b). This deserves a special mention, since this flow was used to calibrate the reference model. Note that there was a small difference between the second and third-order models, but it is difficult to say that the higher order increased the accuracy. Although, at the same time, the WTR canopy model overestimated the shear stress over the vegetation (around 20%, figure 2c). Most likely, this was due to an increased eddy-viscosity (since TKE was larger at the canopy top) and dependent on the value of the  $C_\mu$  coefficient, which remains an open question in the modelling of canopy flows.

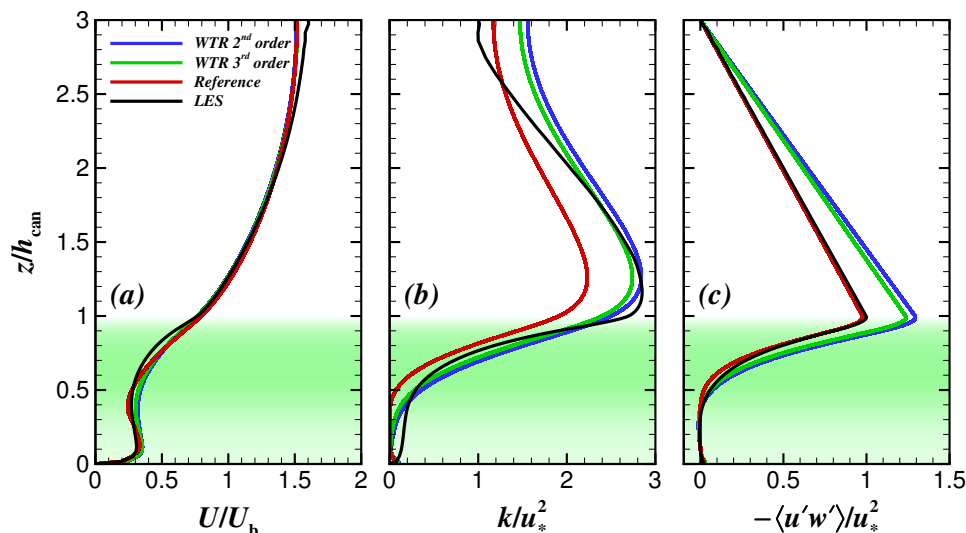


**Figure 2.** *A posteriori* comparison of RaNS  $k-\varepsilon$  canopy models with the large-eddy simulation of the horizontally homogeneous canopy flow. (a) Mean velocity, (b) turbulent kinetic energy and (c) Reynolds shear stress profiles. Data normalized with average wind speed ( $U_b$ ) and friction velocity at the canopy top ( $u_*$ ) in the large-eddy simulation.

In the forest edge flow, the results obtained with the WTR and reference canopy models were very similar (figure 3). It was expected that the WTR canopy model could improve the predictions on the leading edge of the forest, since the flow is out of equilibrium and far from the calibration conditions of the reference model [5], but the results obtained with the RaNS models were almost indistinguishable there and the overestimation of the Reynolds shear stress remains one of the major deficiencies (figure 3c).

The predictions of the flow over the forested hill with the RaNS models were also similar (figure 4). The major deficiency in this case was that both models were unable to predict the separation that occurs in the leeward side of the hill. Although, even in the windward side the RaNS profiles for the mean velocity and TKE changed less across the sections than LES results (figures 4a–b) and the Reynolds shear stress was largely overestimated. Note that, while in the horizontally homogeneous and forest edge flows the turbulence near the ground

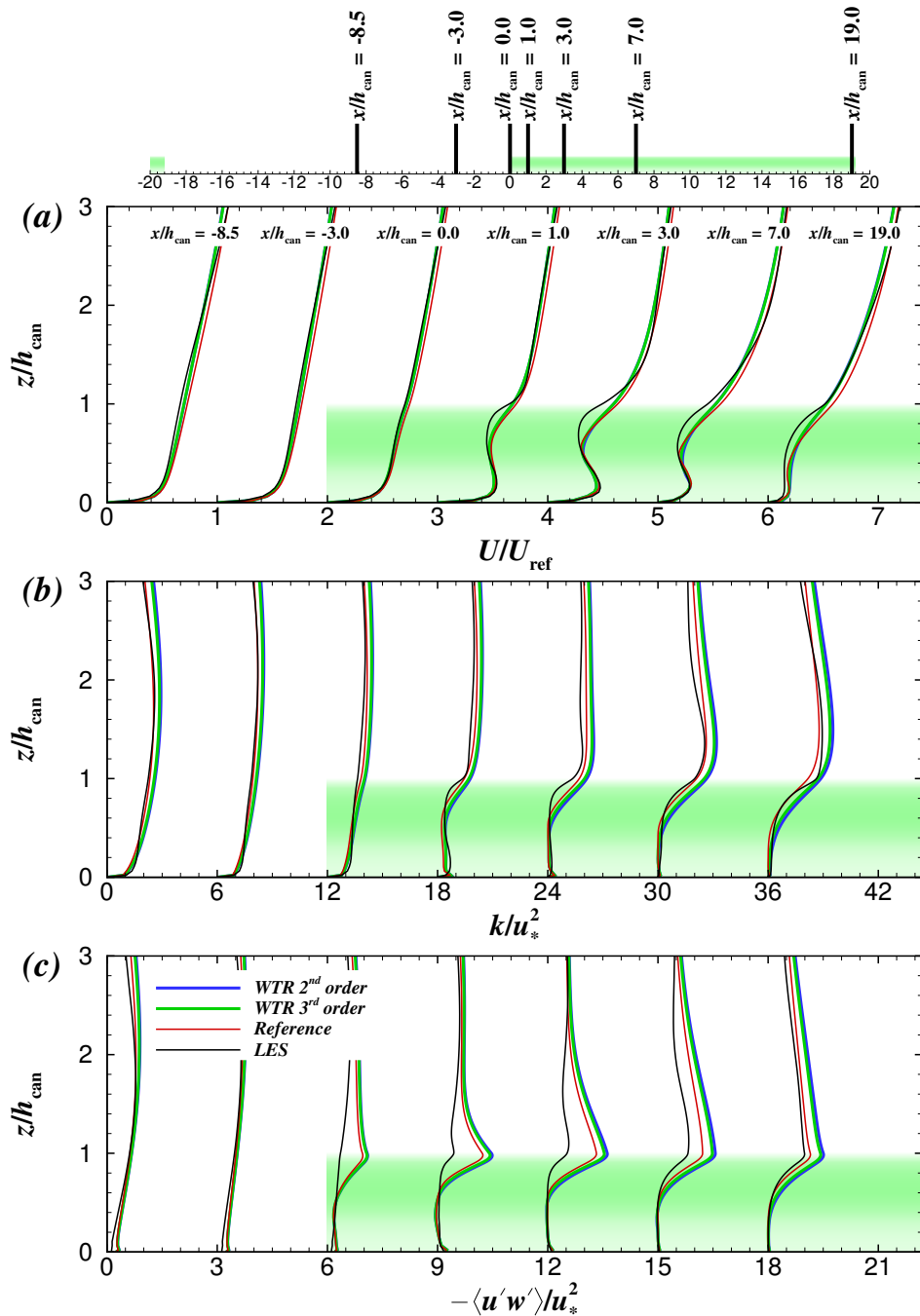


**Figure 3.** *A posteriori* comparison of RaNS  $k-\varepsilon$  canopy models with the large-eddy simulation of the flow across a forest edge. (a) Mean velocity, (b) turbulent kinetic energy and (c) Reynolds shear stress. Data normalized with mean velocity in a flat-plate boundary-layer at  $z/h_{\text{can}} = 2$  ( $U_{\text{ref}}$ ) and friction velocity at the canopy top ( $u_*$ ) in the large-eddy simulation of the flow over a long forest.

was underestimated, here it was always overestimated, a result of the overprediction of TKE production [5].

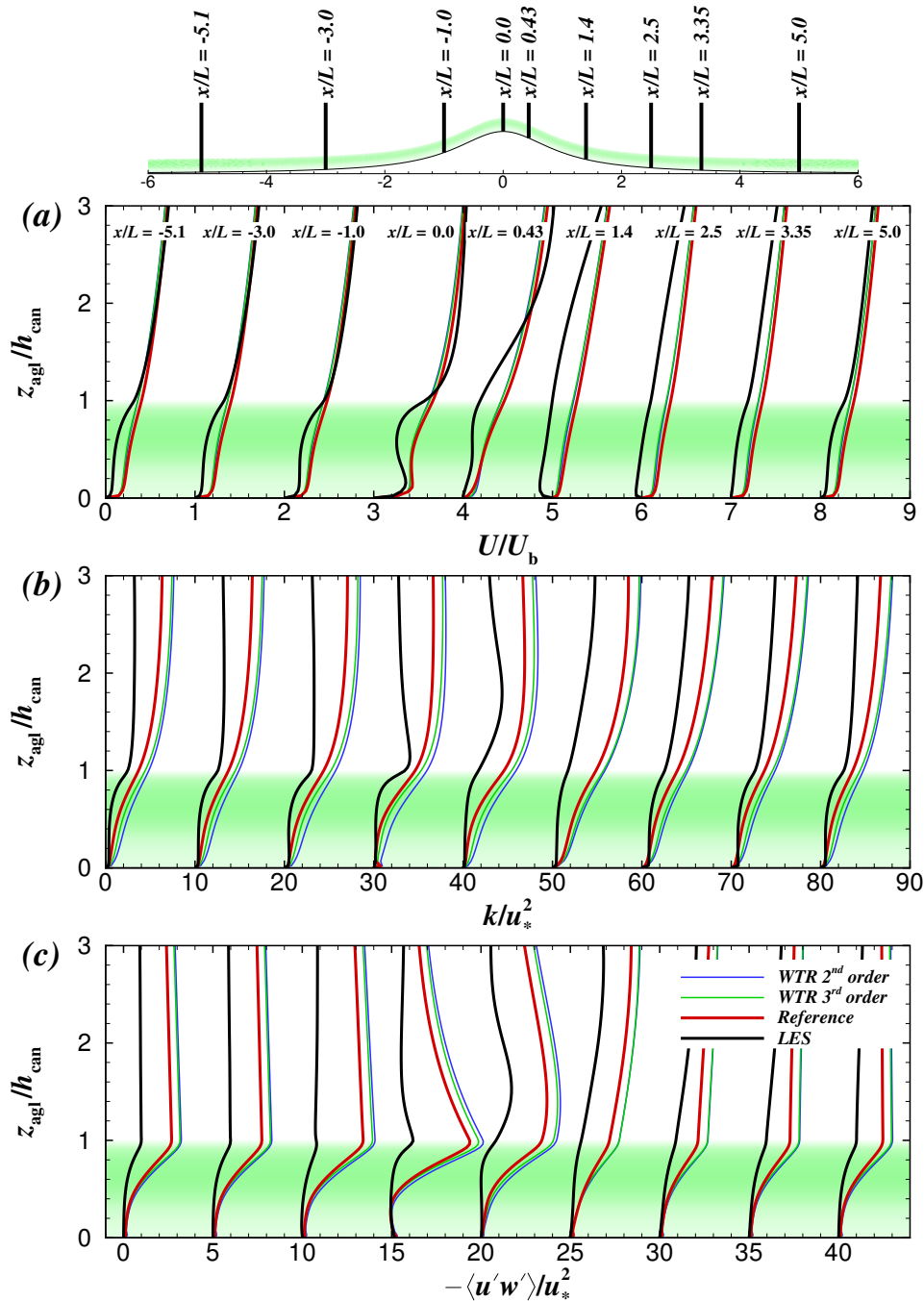


**Figure 4.** *A posteriori* comparison of RaNS  $k-\varepsilon$  canopy models with the large-eddy simulation of the flow over a forested hill. (a) Mean velocity, (b) turbulent kinetic energy and (c) Reynolds shear stress. Data normalized with average wind speed ( $U_b$ ) and friction velocity at the canopy top ( $u_*$ ) at the  $x/L = -3.0$  section of the large-eddy simulation.

## 5. Conclusions

A new model for the vegetation effect on the RaNS transport of turbulent kinetic energy was derived. The model uses a Taylor series expansion of the magnitude of the velocity around a velocity-scale based on the sum of the kinetic energies of the mean and turbulent fields. Using

this expansion and the perturbation theory, it was possible to obtain the contributions to the transport of turbulent kinetic energy as a sum of velocity moments and their spatial gradients.

Using an *a priori* analysis, the model was found to provide better accuracy than traditional models, based mainly on dimensional arguments. However, *a posteriori* comparisons found that the model was usually unable to improve the results of a model based on dimensional arguments and calibrated using large-eddy simulation results. The main deficiencies previously detected remain: turbulence near the ground is usually underestimated and the turbulent kinetic energy production was overestimated in the flow over a forested hill. In this later case, the resultant higher turbulence changed significantly the flow, suppressing the separation in the lee side of the hill. This should not be surprising since these deficiencies were previously related to the  $k-\varepsilon$  model itself and not to the canopy model.

Nevertheless, there was one positive aspect of this study: the results obtained by the new approach were very similar to the ones that were obtained using a traditional model with coefficients calibrated using large-eddy simulation results. Both models are the result of very different approaches to the problem of modelling vegetation, but the fact that they produce such similar results makes us believe in the validity of both and that the deficiencies detected are really due to the original  $k-\varepsilon$  model and not to lack of accuracy in the modelling of vegetation effects.

## References

- [1] Svensson U and Häggkvist K 1990 *Journal of Wind Engineering and Industrial Aerodynamics* **35** 201–211
- [2] Green S R 1992 *The PHOENICS Journal of Computational Fluid Dynamics and its Applications* **5** 294–312
- [3] Liu J, Chen J M, Black T A and Novak M D 1996 *Boundary-Layer Meteorology* **77** 21–44
- [4] Sanz C 2003 *Boundary-Layer Meteorology* **108** 191–197
- [5] Silva Lopes A, Palma J M L M and Viana Lopes J 2013 *Boundary-Layer Meteorology* **149** 231–257
- [6] Mason P J and Thomson D J 1992 *Journal of Fluid Mechanics* **242** 51–78
- [7] Meneveau C, Lund T S and Cabot W H 1996 *Journal of Fluid Mechanics* **319** 353–385
- [8] Launder B E and Spalding D B 1974 *Computer Methods in Applied Mechanics and Engineering* **3** 269–289
- [9] Beljaars A C M, Walmsley J L and Taylor P A 1987 *Boundary-Layer Meteorology* **38** 273–303
- [10] Shaw R H and Schumann U 1992 *Boundary-Layer Meteorology* **61** 47–64
- [11] Yang B, Raupach M R, Shaw R H, Paw U K T and Morse A P 2006 *Boundary-Layer Meteorology* **120** 377–412
- [12] Dupont S, Brunet Y and Finnigan J J 2008 *Quarterly Journal of the Royal Meteorological Society* **134** 1911–1929
- [13] Marusic I, Kunkel G J and Porté-Agel F 2001 *Journal of Fluid Mechanics* **446** 309–320
- [14] Viana Lopes J, Palma J M L M and Silva Lopes A 2016 Modelling the flow within forested areas: the canopy-related terms in the reynolds-averaged formulation To be submitted for publication
- [15] Lien F S, Yee E and Wilson J D 2005 *Boundary-Layer Meteorology* **114** 245–285
- [16] Daly B J and Harlow F H 1970 *Physics of Fluids* **13** 2634–2649